The Journal of Immunology

CCR2-Dependent Dendritic Cell Accumulation in the Central Nervous System during Early Effector Experimental Autoimmune Encephalomyelitis Is Essential for Effector T Cell Restimulation In Situ and Disease Progression

Benjamin D. Clarkson, Alec Walker, Melissa G. Harris, Aditya Rayasam, Matyas Sandor and Zsuzsanna Fabry

J Immunol published online 10 December 2014
http://www.jimmunol.org/content/early/2014/12/10/jimmunol.1401320

The Journal of Immunology is published twice each month by
The American Association of Immunologists, Inc.,
1451 Rockville Pike, Suite 650, Rockville, MD 20852

Print ISSN: 0022-1767 Online ISSN: 1550-6606.

Published December 10, 2014, doi:10.4049/jimmunol.1401320

CCR2-Dependent Dendritic Cell Accumulation in the Central Nervous System during Early Effector Experimental Autoimmune Encephalomyelitis Is Essential for Effector T Cell Restimulation In Situ and Disease Progression

Benjamin D. Clarkson,*,†,‡ Alec Walker,*,† Melissa G. Harris,*,† Aditya Rayasam,§ Matyas Sandor,*,† and Zsuzsanna Fabry*,†

Dendritic cells (DCs)—although absent from the healthy CNS parenchyma—rapidly accumulate within brain and spinal cord tissue during neuroinflammation associated with experimental autoimmune encephalomyelitis (EAE; a mouse model of multiple sclerosis). Yet, although DCs have been appreciated for their role in initiating adaptive immune responses in peripheral lymphoid organ tissues, how DCs infiltrate the CNS and contribute to ongoing neuroinflammation in situ is poorly understood. In this study, we report the following: 1) $CD11c^+$ bone marrow–derived DCs and CNS-infiltrating DCs express chemokine receptor CCR2; 2) compared with $CCR2^{+/+}$ cells, adoptively transferred $CCR2^{-/-}$ bone marrow–derived DCs or DC precursors do not accumulate in the CNS during EAE, despite abundance in blood; 3) $CCR2^{-/-}$ DCs show less accumulation in the inflamed CNS in mixed bone marrow chimeras, when compared with $CCR2^{+/+}$ DCs; and 4) ablation of $CCR2^{+/+}$ DCs during EAE clinical onset delays progression and attenuates cytokine production by infiltrating T cells. Whereas the role of CCR2 in monocyte migration into the CNS has been implicated previously, the role of CCR2 in DC infiltration into the CNS has never been directly addressed. Our data suggest that CCR2-dependent DC recruitment to the CNS during ongoing neuroinflammation plays a crucial role in effector T cell cytokine production and disease progression, and signify that CNS-DCs and circulating DC precursors might be key therapeutic targets for suppressing ongoing neuroinflammation in CNS autoimmune diseases. ***The Journal of Immunology*****, 2015, 194: 000–000.**

Dendritic cells (DCs) are APCs capable of migrating from organ tissues to regional lymph nodes and stimulating T cells to promote both tolerance and immunity to self and foreign Ag acquired in situ. In addition to their role in regulating adaptive immune responses in peripheral lymphoid organ (PLO) tissues, DCs accumulate in inflamed tissues, where they are thought to present MHC class II–restricted Ag to coinfiltrating $CD4^+$ effector T cells (1–3). We and others have shown that DCs accumulate in perivascular spaces and within inflammatory foci in mouse models of stroke, multiple sclerosis, epilepsy, and traumatic brain injury, or after intracerebral injection of Ag or cytokines (4–14). In the context of experimental autoimmune encephalomyelitis (EAE), a mouse model of multiple sclerosis, $CD11b^+CD11c^+$ myeloid DCs, which are derived from blood monocytes, represent the majority of these accumulating DCs (11, 13, 15). Recruitment of immature DCs to the CNS during EAE has also been shown to be dependent upon $\alpha_4\beta_1$ integrin, which binds to VCAM-1 on brain endothelium (16). Ex vivo assays suggest these DCs may be important for cross-presentation of MHC class I–restricted Ag to $CD8^+$ T cells and restimulation of $CD4^+$ T cells with MHC class II–restricted myelin Ag (11, 17, 18). Yet, how these inflammatory DCs home to the CNS remains unclear, and whether these cells are essential tissue APCs for in situ reactivation of CNS-infiltrating T cells is unknown.

Despite much research, no report to date has definitively identified chemokines and chemokine receptors that may contribute to DC migration across the in vivo endothelial blood brain barrier and into the perivascular space of the CNS postcapillary venules. Chemokine receptor CCR2 is expressed on monocytes, monocytoid DC precursors, and circulating blood DCs (19). One recent study found that human monocyte-derived DCs migrate across brain vascular endothelial cells in vitro in response to CCL2 and that DCs were distributed adjacent to CCL2 in the CNS of mice with EAE (20). CCR2 has also been previously implicated in the migration of monocytes and myeloid DCs to inflammatory sites, including infected lung (21–23), psoriasis (19, 24), diabetes mellitus (25), and rheumatoid arthritis (26, 27). In CNS tissues, it was shown that astrocyte-specific overexpression of the CCR2 ligand CCL2 leads to spontaneous asymptomatic accumulation of

*Department of Pathology, School of Medicine and Public Health, University of Wisconsin-Madison, Madison, WI 53792; †Department of Laboratory Medicine, School of Medicine and Public Health, University of Wisconsin-Madison, Madison, WI 53792; ‡Graduate Training Program of Cellular and Molecular Pathology, School of Medicine and Public Health, University of Wisconsin-Madison, Madison, WI 53792; and §Graduate Training Program of Neuroscience, School of Medicine and Public Health, University of Wisconsin-Madison, Madison, WI 53792

Received for publication May 22, 2014. Accepted for publication November 11, 2014.

This work was supported by National Institutes of Health Grants NS37570-01A2, NS076946-01A1, and T32GM081061 (to Z.F.) and American Heart Association Award 12PRE12060020 (to B.D.C.).

Address correspondence and reprint requests to Dr. Zsuzsanna Fabry, Medical Science Center, University of Wisconsin-Madison, 1300 University Avenue, 6130 MSC, Madison, WI 53706. E-mail address: zfabry@wisc.edu

The online version of this article contains supplemental material.

Abbreviations used in this article: BM, bone marrow; BMDC, BM-derived DC; cLN, cervical lymph node; DC, dendritic cell; DPI, day postimmunization; DT, diphtheria toxin; DTR, DT receptor; EAE, experimental autoimmune encephalomyelitis; FLT3L, FLT3-ligand; MMP, matrix metalloproteinase; MOG, myelin oligodendrocyte glycoprotein peptide; MS, multiple sclerosis; PLO, peripheral lymphoid organ; WT, wild-type.

perivascular monocytes in the brain with little infiltration into the CNS parenchyma (28). In relapsing-remitting EAE in Lewis rats, CCL2 expression correlates with disease relapse (29). Similarly, $CCL2^{-/-}$ mice have impaired monocyte recruitment to CNS perivascular spaces during CNS viral infection (30). Consistent with this, $CCR2^{-/-}$ mice are protected from EAE, and bone marrow (BM) chimera experiments revealed that host CCL2 deficiency, but not donor deficiency, protected mice from EAE by reducing the recruitment of monocytes and myeloid DCs (31), suggesting the CCL2–CCR2 axis may be important for myeloid cell recruitment to the perivascular spaces of the inflamed CNS. Additionally, whereas adoptively transferred $CCR2^{-/-}$ T cells are capable of inducing EAE in wild-type (WT) mice, WT T cells are incapable of inducing EAE in $CCR2^{-/-}$ mice. This implies that CCR2 is required on one or more immune cell subsets other than T cells for disease onset (22, 32, 33). However, the potential role of CCR2 in recruiting myeloid DCs to the CNS remains unknown and has been largely overshadowed by the marked amelioration of EAE disease progression associated with reduced monocyte recruitment to CNS in $CCR2^{-/-}$ mice.

Thus, we sought to determine whether CCR2 is directly required for DC recruitment into CNS perivascular space during the onset of neuroinflammation, and whether specific attenuation of DC recruitment to CNS tissues could slow disease progression. We report that both CNS-infiltrating DCs and BM-derived DCs (BMDCs) express CCR2 and migrate across brain endothelium in response to CCL2 in vitro and in vivo, and that $CCR2^{-/-}$ DCs or DC precursors are deficient in their accumulation in the inflamed CNS despite abundance in blood and PLO tissues. Moreover, ablation of $CCR2^{+/+}$ DCs or MHC class $II^{+/+}$ DCs during EAE clinical onset (but not at later time points) delays disease progression. These data suggest that CCR2-dependent DC recruitment to the CNS is essential for restimulation of $CD4^+$ T cells with MHC class II–restricted myelin Ag during onset of EAE, but is dispensable at later time points.

Materials and Methods

Mice and BM chimeras

C57BL/6 WT (stock 000664), B6.129S4-$Ccr2^{tm1Ifc}$/J ($CCR2^{-/-}$, stock 004999), B6.PL-$Thy1^a$/CyJ (Thy1.1, stock 000406), B6.FVB-Tg(Itgax-diphtheria toxin [DT] receptor [DTR]/EGFP)57Lan/J (CD11c-DTR, stock 004509), and B6.Cg-Tg(CAG-DsRed*MST)1Nagy/J (Dsred, stock 006051) mice were obtained from The Jackson Laboratory (Bar Harbor, ME). B6.Cg-Tg(Itgax-Venus)1Mnz/J (CD11c-eYFP) transgenic mice on the C57BL/6 background were a generous gift of M. C. Nussenzweig (Rockefeller University, New York, NY). C57BL/6-Tg (Tcra2D2, Tcrb2D2)1Kuch/J (2D2) TCR-transgenic mice with myelin oligodendrocyte glycoprotein peptide $(MOG)_{35–55}$-$H2^b$–restricted $CD4^+$ T cells were a gift of V. Kuchroo (Brigham and Women's Hospital, Harvard Medical School, Boston, MA). The 2D2 mice were crossed with homozygous $Thy1.1^{+/+}$ or $Dsred^{+/+}$ mice to generate 2D2$Thy1.1^{+/-}$ or 2D2$Dsred^{+/-}$ mice used for adoptive T cell transfer experiments. All F_1 offspring used in experiments were screened for TCR-(Vα3Vβ11) and Dsred or Thy1.1-transgene expression by flow cytometry on immune cells isolated from blood. Standard PCR screening was used for CD11c-eYFP (5′-tgc tgg ttg ttg tgc tgt ctc atc-3′, 5′-ggg ggt gtt ctg ctg gta gtg gtc-3′), CD11c-DTR (5′-ggg acc atg aag ctg ctg ccg-3′, 5′-tca gtg gga att agt cat gcc-3′), and $CCR2^{-/-}$ (WT, 5′-cca cag aat caa agg aaa tgg-3′, 5′-cca atg tga tag agc cct gtg-3′; mutant, 5′-ctt ggg tgg aga ggc tat tc-3′, 5′-agg tga gat gac agg aga tc-3′) mice. CD11c-eYFP mice were bred and backcrossed with $CCR2^{-/-}$ mice to generate $CCR2^{-/-}$.CD11c-eYFP mice. For preparation of chimeric mice by BM transplantation, WT mice were irradiated (950 rad) and injected with a mixture of BM cells ($10–15 \times 10^6$, i.v.) from WT, $CCR2^{-/-}$, CD11c-eYFP, $CCR2^{-/-}$CD11c-eYFP, or CD11c-DTR mice 4–10 h after irradiation. All animal procedures used in this study were conducted in strict compliance with the National Institutes of Health *Guide for the Care and Use of Laboratory Animals* and approved by the University of Wisconsin Center for Health Sciences Research Animal Care Committee.

Induction of EAE

EAE was induced as previously described (34). Briefly, emulsion of equal volumes of CFA and 100 μg $MOG_{35–55}$ (MEVGWYRSPFSRVVHLYRNGK) supplemented with *Mycobacterium tuberculosis* H37Ra (5 mg/ml; Difco, Detroit, MI) was injected s.c. in the scapular region of each mouse. MOG-CFA mixture was emulsified by sonication using an ultrasonic homogenizer (Model 300VT equipped with a titanium cup tip; Biologics, Manassas, VA). Pertussis toxin (200 ng/mouse, i.p.) was injected on days 0 and 2 relative to immunization. Clinical scores were monitored daily in a blinded manner and recorded as follows: 0, no clinical disease; 1, flaccid tail; 2, gait disturbance or hind limb weakness; 3, hind limb paralysis and no weight bearing on hind limbs; 4, hind limb paralysis with forelimb paresis and reduced ability to move around the cage; and 5, moribund or dead. The mean daily clinical score and SEM were calculated for each group. The significance of differences was calculated by Student's *t* and Wilcox tests, as described elsewhere (35).

Histology

For fluorescent microscopy, CNS tissues were fixed overnight in 3% formalin/25% sucrose, embedded in OCT compound (Tissue-Tek Sakura, Torrance, CA), and stored at −80˚C. Cryosections (5–10 μm) were cut from OCT-embedded tissue samples, postfixed for 20 min in ice-cold acetone, and washed with PBS (25–50 min). Sections were mounted with ProLong Gold antifade reagent (Invitrogen, Carlsbad, CA) with DAPI. Fluorescent images were acquired at original magnification ×40–400 with Picture Frame software (Optronics) using an Olympus BX41 microscope (Leeds Precision Instruments) equipped with a camera (Optronics, Goleta, CA). For bright field microscopy, CNS tissues were postfixed in 10% formalin and embedded in paraffin for sectioning (10 μm). Tissue sections were stained with H&E or luxol fast blue to detect infiltrating cells or demyelination, respectively. Bright-field images were acquired at ×40–400 final original magnification with Q-Capture software using an Olympus BX40 microscope equipped with a Q-Color 3 camera (Olympus America). Digital images were processed and analyzed using Photoshop CS4 software (Adobe Systems). Color balance, brightness, and contrast settings were manipulated to generate final images. All changes were applied equally to entire image.

Mononuclear cell isolation

For immune cell isolation from CNS tissues, brains and spinal cords were removed from saline-perfused mice, weighed, minced, and incubated with collagenase type IV (1mg/ml) and DNase (28 U/ml) at 37˚C for 45 min. Samples were further homogenized by trituration and filtered through 70-μm cell strainers. The cell suspension was washed with HBSS, resuspended in 70% Percoll (Pharmacia, Piscataway, NY), and overlaid with 30% Percoll. The gradient was centrifuged at 2500 rpm ($625 \times g$) for 30 min at 4˚C without break. Mononuclear cells were collected from the gradient interface and washed once for further analysis. For immune cell isolation from PLO tissues, spleen and cervical lymph nodes were gently dissociated between frosted slides and passed through 70-μm cell strainers. Blood cells were collected transcardially using an insulin syringe (28 g) and transferred into 100 vol 10 mM EDTA HBSS. RBCs were removed from spleen and blood samples using ammonium chloride potassium carbonate RBC lysis buffer and repeated washing.

Intracellular cytokine staining and flow cytometry

For ex vivo recall responses, single-cell suspensions from various tissues were cultured at 37˚C in 10% FBS in RPMI 1640 media containing GolgiStop (BD Biosciences, San Jose, CA) with or without additional stimulating agents, including PMA (50 ng/ml) and ionomycin (1 μg/ml), $MOG_{35–55}$ peptide (2–20 μg/ml), or anti-CD3 (1 μg/ml)/anti-CD28 (2 μg/ml) for 5 h. For immune-fluorescent labeling, 10^6 cells isolated from CNS and PLO tissues were incubated for 30 min on ice with saturating concentrations of fluorochrome-labeled mAbs. Unlabeled 2.4G2 mAb (40 μg/mL) was used to block nonspecific binding of fluorochrome-labeled mAbs to Fc receptors. After staining, cells were washed three times using FACS buffer (1% BSA in PBS). For intracellular staining, cell suspensions were then fixed and permeabilized overnight (4˚C) with Cytofix/Cytoperm solution (BD Biosciences). The next day, cells were washed with Perm/Wash buffer (BD Biosciences) and stained with mAbs against IFN-γ and IL-17. Fluorochrome-labeled mAbs against CD45 (30-F11), CD11b (M1/70), CD11c (HL3), CD80 (16-10A1), CD86 (GL1), CD40 (3/23), PDL1 (MIH5), PDL2 (Ty25), $I\text{-}A^b$ (AF6-120.1), B220 (RA3-6B2), CD4 (RM4.5), Vβ11 (RR3-15), Thy1.1 (OX7), CD8a (53-6.7), IFN-γ (XMG1.2), IL-17 (TC11-18H10), and appropriate isotype controls were purchased from BD Biosciences (Minneapolis, MN). Anti-CCR2 Ab

(clone 475301, anti-mouse/rat CCR2 rat IgG2b) was obtained from R&D Systems (Minneapolis, MN). Fluorochrome-labeled mAbs against CD45.1 (A20) and CD45.2 (104) were purchased from eBioscience (San Diego, CA). Cell staining was acquired on a FACSCalibur or LSRII (BD Biosciences) and analyzed with FlowJo (Tree Star) software version 10.0.6.

BMDC differentiation

DCs were generated, as previously described (9). Briefly, BM cell suspensions obtained from femurs and tibias of C57BL/6 mice were resuspended in ACK-containing RBC lysis buffer to remove erythrocytes, washed, and plated in RPMI 1640 with 20% FBS supplemented with 100 U/ml penicillin/streptomycin and GM-CSF or FLT3-ligand (FLT3L). GM-CSF and FLT3L were titrated from supernatants of the GM-CSF–secreting X-63 (gift of A. Erdei, Eotvos University, Budapest, Hungary) or FLT3L-secreting Chinese hamster ovary cell lines (generated by N.A. Nicola, generous gift of M. Nussenzweig, The Rockefeller University). In GM-CSF–containing cultures, nonadherent and loosely adherent DC precursors were removed and replated in a new flask after 6 d in culture. DCs were collected and used for experiments between 9 and 13 d of culture. For Ag pulse, DCs were cultured with or without $MOG_{35–55}$ peptide (10 μg/ml) and LPS (500 ng/mL) for 4 h. After pulsing, cells were washed extensively before use.

T cell purification and adoptive transfer

For adoptive transfer of 2D2 T cells, 2D2 mice were immunized with 100 μg $MOG_{35–55}$ emulsified in CFA, and lymphocytes were isolated from PLO tissues 7 d later. To enrich for $CD4^+$ T cells prior to FACS sorting, cells were stained with biotinylated mAbs against CD11b (M1/70) and B220 (RA3-6B2). Cells were then washed, incubated with streptavidin microbeads, and separated on a MidiMACS separator using LD columns, according to the manufacturer's instructions (Miltenyi Biotec, San Diego, CA). After negative selection, cells were stained with fluorochrome-labeled mAbs against CD4 (RM4.5), Vβ11 (RR3-15), Thy1.1 (OX7), CD44 (IM7), LFA-1 (2D7), and CD62L (MEL-14), before undergoing FACS on a FACSAria II SORP at the University of Wisconsin Carbone Cancer Center Flow Cytometry Laboratory. T cells were collected in FBS containing media, washed with PBS, and transferred (i.v.) into recipients by retro-orbital injection (200 μl; naive T cells, 5×10^6 cells/mouse; effector T cells, 1×10^6 cells/mouse).

DC ablation with DT

To ablate $CD11c^+$ DCs, DT (625 ng/kg, 500 μl, i.p.; List Biological Laboratories, Campbell, CA) was injected into CD11c-DTR mixed BM chimera mice. DC ablation was consistently ∼90% efficient (data not shown). Ablation was maintained by repeating the injection every 48 h for up to 6 d. No mouse received more than four injections of DT. All mice weighed ∼20–25 g upon EAE induction and were monitored for clinical score and body condition scoring starting at day 7. If noticeable weight loss was observed following DT treatment, animals were weighed and excluded from analysis if they had lost >20% of their body mass. In our hands, DT treatment was not associated with noticeable weight loss.

Statistical analyses

Results are given as means ± 1 SD. Multiple comparisons were made using one-way ANOVA. Where appropriate, two-sided Student's *t* test analysis was used to compare measures made between two groups. The *p* values <0.05 were considered significant.

Results

Ablation of $Cd11c^+$ DCs during preclinical EAE ameliorates disease

In the context of EAE, DCs are thought to be important for T cell priming and the initiation of adaptive immunity to myelin Ags in PLO tissues. However, T cells also require TCR restimulation within the CNS perivascular space to enter the CNS parenchyma (36, 37). Myeloid DCs have also been shown to accumulate in the CNS preclinically and during disease onset (13, 15, 20) in which they express MHC class II and form close interactions with T cells (3, 11). Yet, because other APCs such as perivascular macrophages also accumulate within the CNS and interact with T cells (38, 39), whether DCs are essential APCs during the effector phase of EAE is controversial. To address this question, we induced EAE in mice expressing the human DTR downstream of the DC-associated CD11c promoter and administered DT during disease onset or during peak disease. DTR expression in a majority of $CD11c^+$ DCs allowed for transient ablation of >90% of $CD11c^+$ DCs in CNS and PLO tissues for 48 h following administration of DT (625 ng/kg, i.p.) (Fig. 1A, Supplemental Fig. 1). As shown in Fig. 1B, DC ablation during disease onset delayed and partially ameliorated EAE clinical course. In contrast, mice treated with DT during peak disease maintained higher clinical scores than PBS-treated control mice, but these differences were not statistically significant. These data suggest that DCs may differentially contribute to or regulate onset and progression of neuroinflammation at different time points during disease. Specifically, the amelioration of EAE clinical scores in mice treated with DT prior to disease onset highlighted the essential role of DCs—potentially as proinflammatory APCs during this time period when these cells first begin to accumulate in the CNS (15, 40) (our unpublished observations).

$CD11c^+$ BMDCs and CNS-infiltrating DCs express CCR2, and CCR2 contributes to BMDC infiltration into the inflamed CNS

CCR2 has been implicated in monocyte migration from blood and BM into tissues. Thus, we sought to determine the role of CCR2 in DC recruitment to the CNS during neuroinflammation. We observed a dose-dependent increase in migration of BMDCs across mouse brain endothelial cell monolayers in response to CCL2, as previously reported (20) (Fig. 2A). Similarly, we found that relative to mice intracerebral injected with PBS, mice that received intracerebral injections of CCL2 exhibited an increased frequency of brain-infiltrating myeloid cells (CD45-high $CD11b^+$) and DCs (CD45-high $CD11b^+CD11c^+$), but not microglia (CD45-low CD11b) (Fig. 2B). Flow cytometry of cells isolated from CNS and peripheral lymphoid organ tissues during EAE also confirmed the expression of the CCR2 on $CD11b^+CD11c^+$ brain infiltrates and splenocytes (Fig. 2C). As in vitro differentiated BMDCs express high level of CCR2 (Fig. 2D, *left column*), we decided to further test the direct role of CCR2 in DC recruitment to the inflamed CNS. We cultured BMDCs from CCR2-sufficient ($CCR2^{+/+}$)/CD11c-eYFP and congenic CCR2-deficient ($CCR2^{-/-}$)/CD11c-eYFP mice and transferred equal numbers of these cells (25×10^6/mouse) into congenic WT colorless recipients with active clinical disease at day post-immunization (DPI) 12–13. Cells from CNS and PLO tissues were isolated 4 d later to compare BMDC recruitment. As shown, $CCR2^{+/+}$ and $CCR2^{-/-}$ BMDCs expressed similar levels of the eYFP transgene on the day of transfer (Fig. 2D, *left column*). We observed no difference in the expression of CD11b or costimulatory markers between $CCR2^{+/+}$ and $CCR2^{-/-}$ BMDCs (data not shown). At peak disease (DPI 16–17), the frequency of CD11c-$eYFP^+$ BMDCs in spleens (Fig. 2D) and cervical lymph nodes (cLN; data not shown) did not differ between mice receiving $CCR2^{+/+}$ and $CCR2^{-/-}$ BMDCs. In contrast, at this time point, higher numbers of $CCR2^{+/+}$ CD11c-$eYFP^+$ BMDCs were present in inflamed CNS tissues compared with their $CCR2^{-/-}$ counterparts (Fig. 2D). Interestingly, mice receiving $CCR2^{+/+}$ BMDCs during early disease exhibited larger increases in clinical scores when assessed 2–4 d later (Fig. 2D, 2E), suggesting that—much as ablating DCs during this time period can delay EAE clinical progression—increasing the frequency of circulating $CD11c^+$ DCs during this time frame can accelerate disease progression. To control for the potentially confounding influence of endpoint clinical score on BMDC recruitment, we also compared recruitment of $CCR2^{+/+}$ and $CCR2^{-/-}$ BMDCs to CNS tissues, grouping mice with similar clinical scores. Even within these constraints, we saw a higher frequency of $CCR2^{+/+}$ BMDCs in CNS tissues compared with $CCR2^{-/-}$ BMDCs (Fig. 2E). These

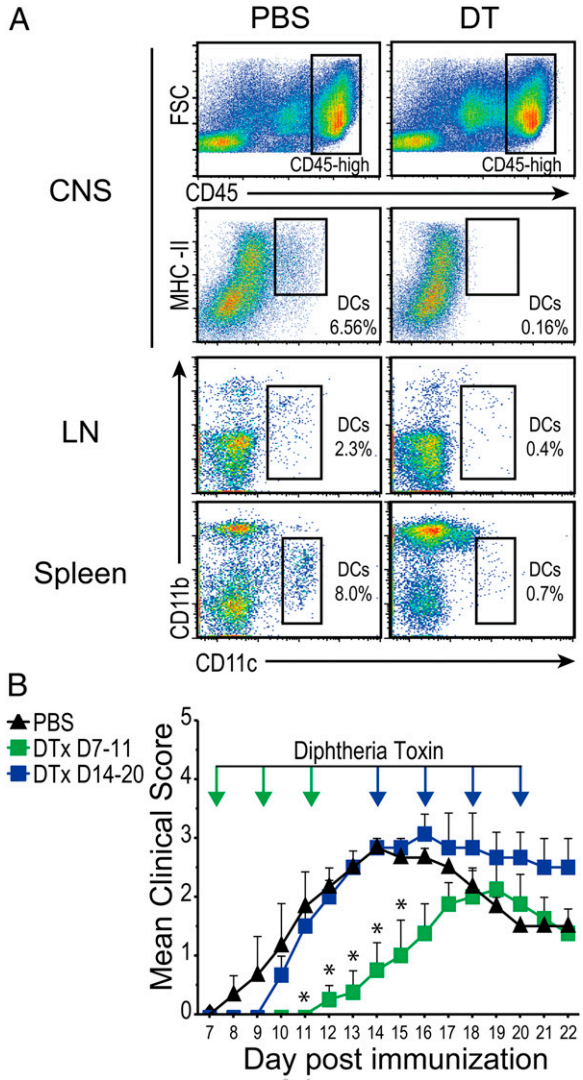

FIGURE 1. Ablation of CD11c$^+$ DCs during preclinical EAE clinical delays disease progression. (**A**) CD11c-DTR mice were injected with DT (625 ng/kg, i.p.) or PBS control, and 24–48 h later immune cells were isolated from CNS tissues, spleen, and pooled lymph nodes (axial, mesenteric, cervical). CNS tissues were harvested from mice with EAE on day 13 postimmunization (receiving i.p. injections of DT on days 7, 9, and 11). Representative dot plots show CD11b and CD11c expression on CD45-high gated leukocytes (above). Numbers indicate percentage of cells in boxed gate. Data representative of two independent experiments with $n = 3$ mice per group. (**B**) Mean clinical scores in CD11c-DTR mice following EAE induction by $MOG_{35–55}$ immunization. CD11c$^+$ cells were ablated on days 7, 9, and 11 (green lines) or days 14, 16, 18, and 20 (blue lines) by administration of DT (625 ng/kg, i.p.). Data representative of two independent experiments with n = 3–5 mice per group. Error bars indicate SEM. *$p < 0.05$, Student t test.

data provide direct evidence that CCR2 expressed on DCs promotes recruitment of these cells to the inflamed CNS.

Compared with CCR2$^{+/+}$ cells, adoptively transferred CCR2$^{-/-}$ DC precursors do not accumulate in the CNS during EAE, despite abundance in blood

To further understand the role of CCR2 in regulating CD11c$^+$ cell migration into the CNS in vivo, we induced EAE in CCR2$^{+/+}$ mice expressing Dsred fluorescent protein ubiquitously under the CAG promoter (CD45.2$^{+/+}$CCR2$^{+/+}$Dsred$^{+/+}$), as well as in CCR2$^{-/-}$ colorless mice (CD45.2+CCR2$^{-/-}$Dsred$^{-/-}$) and CD45.1$^{+/+}$ colorless mice. At DPI 12 or 16, we transferred 50/50 mixtures of BM cells from CD45.2$^{+/+}$CCR2$^{-/-}$Dsred$^-$ and CD45.2$^{+/+}$CCR2$^{+/+}$ Dsred$^+$ donor mice into congenic CD45.1$^{+/+}$ recipients with synchronous EAE (10–15 $\times$ 10^6/mouse, i.v.). Four days later, we isolated immune cells from CNS and PLO tissues and analyzed the frequency of CCR2$^{+/+}$ (Dsred$^+$) and CCR2$^{-/-}$ (Dsred$^-$) cells among CD45.2$^+$ CD11b$^+$CD11c$^+$ donor-derived DCs by flow cytometry. We first gated on CD45.2$^+$CD45.1$^-$ cells (Fig. 3A) and then gated on CD11b$^+$ CD11c$^+$ cells to compare the relative frequency of CCR2$^{+/+}$ (Dsred$^+$) and CCR2$^{-/-}$ (Dsred$^-$) donor-derived DCs in BM, blood, spleen, and CNS (gating shown in Fig. 3D). At both end points (DPI 16 and DPI 20), we observed similar frequencies of CCR2$^{+/+}$ and CCR2$^{-/-}$ DCs in spleen, with elevated relative frequencies of CCR2$^{-/-}$ DCs in both BM and blood (Fig. 3C). Despite the relatively high level of CCR2$^{-/-}$ DCs observed in circulation, we detected a much lower frequency of CCR2$^{-/-}$ DCs in CNS tissues relative to CCR2$^{+/+}$ DCs, especially at the earlier time point (DPI 12–16). To illustrate this point, we also present the relative frequency of CCR2$^{+/+}$ and CCR2$^{-/-}$ DCs in blood and CNS of individual recipient mice (Fig. 3B). In all cases, CCR2$^{-/-}$ DCs were present at lower frequencies in CNS tissues relative to their frequency among donor cells in the blood of the same mouse. The reciprocal was true of CCR2$^{+/+}$ DCs, which were present at higher frequencies in CNS tissues than in blood of all animals (mean difference 61.8% $\pm$ 10.9%, DPI 12–16; 37% $\pm$ 12.3%, DPI 16–20). These studies provide strong evidence that CCR2 is crucial for DC recruitment to the inflamed CNS, at least within the limited time frames under which we could study this phenomenon in vivo.

CCR2$^{-/-}$ DCs show less accumulation in the inflamed CNS in mixed BM chimera when compared with CCR2$^{+/+}$ DCs

Next, we generated mixed BM chimera mice, wherein we could track CCR2-dependent DC recruitment to the CNS throughout the course of EAE onset. We reconstituted WT (C57BL/6) mice with a 50/50 mixture of WT BM cells and BM cells from either congenic CCR2$^{-/-}$CD11c-eYFP or CCR2$^{+/+}$CD11c-eYFP mice. After reconstitution and recovery, we immunized these mice with $MOG_{35–55}$/CFA to induce EAE. We isolated immune cells from CNS and PLO tissues from these mice 8, 12, and 16 d later to compare recruitment of CCR2$^{+/+}$ and CCR2$^{-/-}$ CD45$^+$ CD11c-eYFP cells (gating shown in Fig. 4A). As expected, due to the presence of a partially WT hematopoietic system, no difference in the onset or severity of EAE was observed between mice in these groups (data not shown). We also observed similar levels of CD11c-eYFP$^+$ cells in both spleen and cLNs of CCR2$^{+/+}$CD11c-eYFP and CCR2$^{-/-}$ CD11c-eYFP BM recipients (Fig. 4C). In sharp contrast, as early as DPI 12, we saw markedly reduced accumulation of CCR2$^{-/-}$ CD11c-eYFP$^+$ cells in CNS relative to CCR2$^{+/+}$CD11c-eYFP$^+$ cells. To assess regional differences in DC recruitment, we dissected CNS anatomical regions prior to immune cell isolation and flow cytometric analysis. By this method, we found that, whereas the frequency of host-derived radioresistant microglial cells (CD45-low CD11b$^+$) did not differ between groups in most regions, the frequency of donor-derived CD11c-eYFP$^+$CD45-high cells was markedly lower in CCR2$^{-/-}$CD11c-eYFP recipients in all CNS tissues analyzed, save hippocampus. These differences in recruitment persisted or increased in all CNS anatomical regions by DPI 16 (Fig. 4B).

Further investigation of the in situ distribution of these CD11c-eYFP$^+$ cells by fluorescent microscopy revealed that the majority of CD11c-eYFP$^+$ cells found in the CNS of CCR2$^{-/-}$CD11c-eYFP recipients were restricted to the choroid plexus of the lateral and third ventricles adjacent to the hippocampus. A minority of CD11c-eYFP$^+$ cells in these mice were also found in the taenia tecta and the islands of Calleja on the ventral side of the olfactory

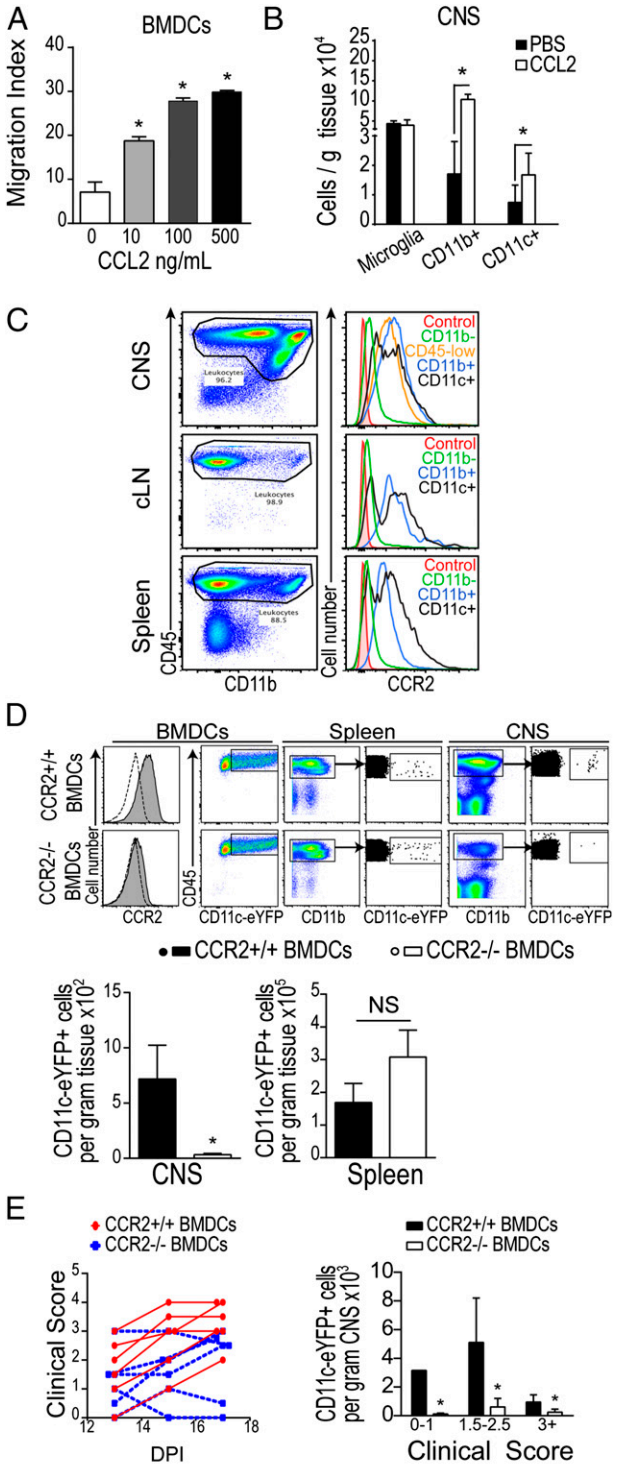

FIGURE 2. CD11c$^+$ BMDCs and CNS-infiltrating DCs expressing CCR2 and CCR2 contribute to BMDC infiltration into the inflamed CNS. (**A**) Migration of GFP$^+$ BMDCs across mouse brain endothelial cell monolayers into lower compartments of single-layer Transwell artificial blood brain barrier models in response to dose curve of CCL2. Measurements were made by flow cytometry and quantified relative to number of nonfluorescent loading-control cells (added directly to lower chamber). (**B**) Column graphs show absolute number of CD45-low CD11b$^+$ microglia, infiltrating myeloid cells (CD45-high CD11b$^+$), and DCs (CD45-high CD11b$^+$ CD11c$^+$) in the ipsilateral hemisphere of mice intracerebrally injected, as indicated. (**C**) CCR2 expression on indicated cell populations isolated from CNS tissues of C57BL/6 mice with MOG-induced EAE (DPI 12). CD11c$^+$ cells were gated from CD11b$^+$ population. (**D**) BMDCs generated from CCR2$^{-/-}$CD11c-eYFP or CCR2$^{+/+}$CD11c-eYFP mice were transferred (25×10^6, i.p.) into WT C57BL/6 mice with ongoing MOG-induced EAE (DPI 12–13). Histograms show CCR2 expression on BMDCs before transfer. Dot plots show CD11c-eYFP$^+$ cells among BMDCs before transfer and among CD45$^+$ immune cells isolated from spleen and CNS tissue 4 d later (quantified below). Data representative of two independent experiments with n = 3–6 mice per group. (**E**) Clinical scores in individual BMDC recipient mice from (C). Frequency of CD11c-eYFP$^+$ cells in CNS of CCR2$^{+/+}$ BMDC and CCR2$^{-/-}$ BMDC recipients with similar clinical scores. Error bars indicate SEM. *$p < 0.05$, Student t test.

tubercle (Fig. 4D). In contrast, CCR2$^{+/+}$CD11c-eYFP recipients exhibited disseminated infiltration of CD11c-eYFP$^+$ cells throughout the CNS, with prominent infiltrates in the white matter tracks of the cerebellum, the cerebral cortex, and ventral portions of the olfactory bulb, as well as the ventricles and surrounding neuropil of the hippocampus and superior colliculus (Fig. 4D). These studies confirmed that CCR2 is required for DC recruitment to the CNS, but not PLO tissues during EAE.

Ablation of CCR2$^{+/+}$ DCs during EAE clinical onset delays progression

To explore the functional consequences of DC recruitment to CNS tissues on disease progression, we generated mixed BM chimera mice in which we could transiently ablate CCR2$^{+/+}$ DCs and thereby diminish DC recruitment to the CNS. We generated mixed BM chimeric mice by reconstituting irradiated WT mice with BM cells from congenic CD11c-DTR mice and BM cells from CCR2$^{-/-}$ or CCR2$^{+/+}$ mice. These mice are referred to hereafter as CCR2$^{-/-}$:CD11cDTR mice and CCR2$^{+/+}$:CD11cDTR mice. After reconstitution and recovery, we immunized these mice with MOG/CFA to induce EAE and administered DT (625 ng/kg, i.p.) during disease onset (DPI 8–12) or during peak disease (DPI 14–18) to ablate CD11c-DTR$^+$ DCs. When we administered DT during peak disease, we observed no difference between CCR2$^{+/+}$:CD11c-DTR and CCR2$^{-/-}$:CD11c-DTR mice in subsequent clinical scores or effector T cell cytokine production within the CNS (data not shown). In contrast, when we ablated CD11c-DTR$^+$ DCs during clinical onset, DT-treated CCR2$^{-/-}$:CD11c-DTR mice exhibited a significant delay in clinical progression compared with either DT-treated CCR2$^{+/+}$:CD11c-DTR BM recipients or PBS-treated CCR2$^{-/-}$:CD11c-DTR recipients (Fig. 5A). Ablation of CD11cDTR$^+$ DCs also correlated with reduced levels of IFN-γ– and IL-17–producing CD4$^+$ T cells as well as reduced levels of IFN-γ–producing CD8$^+$ T cells in the brain and spinal cord of these mice relative to controls (Fig. 5B). Further examination of spinal cord tissues revealed a reduced number of inflammatory foci and demyelinated lesions in mice with ablated CCR2$^{+/+}$ DCs (micrographs shown in Fig. 5D; demyelination quantified in Fig. 5C). These data indicate that CCR2-dependent recruitment of CD11c$^+$ DCs to CNS tissues during onset of EAE critically contributes to CNS-infiltrating T cell cytokine production and EAE disease pathology.

Preclinical ablation of MHC class II$^+$ DCs prevents recruitment of Ag-experienced encephalitogenic T cells to CNS and ameliorates EAE

Once they have infiltrated the CNS, CD4$^+$ T cells must first reencounter their cognate Ag in the context of MHC class II molecules on local APCs to carry out effector functions, such as cytokine secretion (36, 37, 41). Thus, to explore the potential role of DCs as tissue APCs that might contribute to T cell restimulation in situ, we analyzed the relative localization of CNS-infiltrating DCs and T cells. We purified MOG-specific CD4$^+$ T cells from TCR transgenic 2D2 mice bred onto a Dsred background (2D2.Dsred)

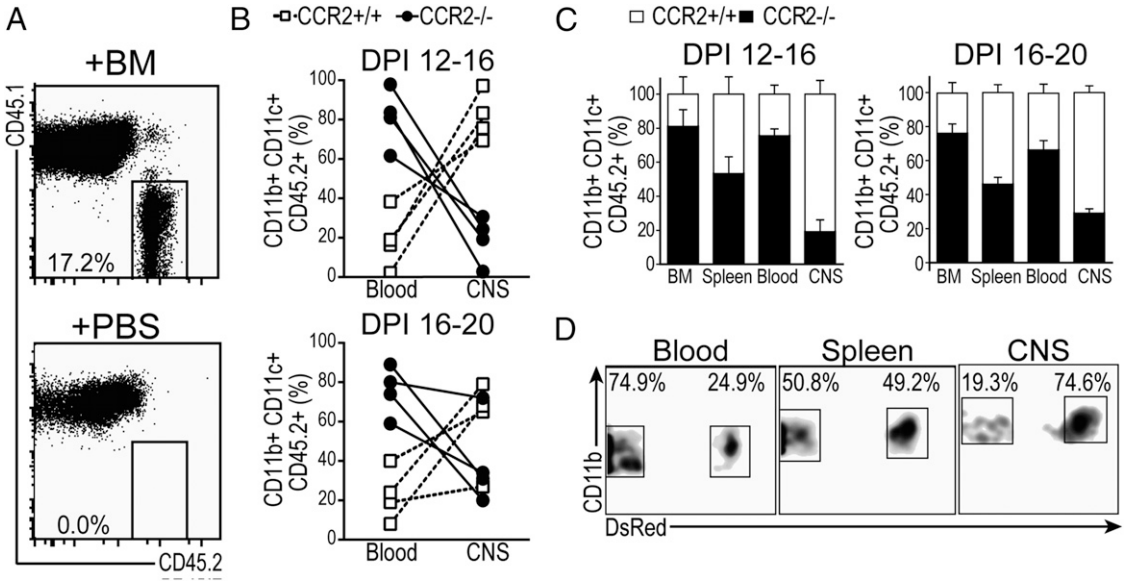

FIGURE 3. CCR2$^{-/-}$ DCs do not accumulate in inflamed CNS despite abundance in blood. CD45.2$^+$ BM cells were adoptively transferred into CD45.1$^+$ hosts at day 12 or 16 of EAE, and mice were euthanized for tissue collection 4 d later at day 16 or 20, respectively. (**A**) Flow plots showing spleen cells from CD45.1 mice adoptively transferred with either PBS or equal mixtures of BM from CD45.2$^{+/+}$CCR2$^{+/+}$ DsRed$^+$ and CD45.2$^{+/+}$CCR2$^{-/-}$ DsRed$^+$ mice. (**B**) Frequency of CCR2$^{+/+}$ (Dsred$^+$) and CCR2$^{-/-}$ (Dsred$^-$) among donor (CD45.2$^+$) cells in blood and CNS. Lines indicate difference in frequency in blood and CNS from individual mice. (**C**) Frequency of CCR2$^{+/+}$ (Dsred$^+$) and CCR2$^{-/-}$ (Dsred$^-$) among donor (CD45.2$^+$) cells in BM, spleen, blood, and CNS at days 16 and 20 of EAE. Data are representative of three independent experiments with $n = 3$ mice per group. Error bars indicate SEM. (**D**) Representative flow plots showing percentage of cells CCR2$^{+/+}$ (Dsred$^+$) and CCR2$^{-/-}$ (Dsred$^-$) among donor (CD45.2$^+$CD45.1$^-$) CD11b$^+$ and CD11c$^+$ cells in blood, spleen, and CNS of mice from (A). Data are representative of three independent experiments with $n = 3$ mice per group.

and transferred these cells into CD11c-eYFP mice prior to EAE induction by MOG immunization to visualize the in situ localization of CNS-infiltrating encephalitogenic MOG-specific 2D2, Dsred and coinfiltrating CD11c-eYFP$^+$ DCs by fluorescent microscopy. As shown in Fig. 6A, both MOG-specific CD4$^+$ T cells and CD11c-eYFP$^+$ cells accumulated within the ventricles and surrounding tissues of the CNS at the time of clinical onset (DPI 12). We observed extensive colocalization of these cells within the CNS (our unpublished data), suggesting these cells may form functional interactions in situ.

To determine whether these colocalizations could represent functional T cell–APC (TCR–Ag–MHC class II) interactions, we analyzed CNS leukocyte subsets for the expression of MHC class II by flow cytometry. Whereas CD11c$^+$ cells represented a minority of total leukocytes within inflamed CNS tissues, CD11c$^+$ cells exhibited higher frequencies of MHC class II$^+$ cells than CD11c$^-$ cells among both CD11b$^+$ and CD11b$^-$ cell subsets (Fig. 6B)—indicating that CNS-infiltrating CD11c$^+$ cells are well equipped to regulate the activity of coinfiltrating CD4$^+$ T cells through MHC class II–Ag–TCR interactions. This is consistent with a recent study showing higher expression of MHC class II on CD11c$^+$ than CD11c$^-$ cells (42). Thus, to explore this potential, we generated mixed BM chimera mice in which we could transiently ablate MHC class II$^{+/+}$ DCs. We reconstituted irradiated WT mice with 50/50 mixtures of congenic CD11c-DTR BM cells and BM cells from either MHC class II$^{-/-}$ or MHC class II$^{+/+}$ mice. After reconstitution and recovery, we immunized these mice with MOG/CFA to induce EAE and administered DT (625 ng/kg, i.p.) during disease onset (DPI 8–12). As shown, we observed normal disease onset in both DT-treated MHC class II$^{+/+}$:CD11c-DTR BM recipients as well as PBS-treated MHC class II$^{-/-}$:CD11c-DTR BM recipients. However, clinical onset was comparatively delayed and partially ameliorated in DT-treated MHC class II$^{-/-}$:CD11c-DTR BM recipient mice (Fig. 6C). This was associated with reduced frequency of IFN-γ–producing and IL-17–producing CD4$^+$ MOG-specific T cells in the CNS at peak disease (DPI 16, Fig. 6D)—indicating that MHC class II–dependent Ag presentation by CD11c$^+$ DCs is required after initial T cell priming for disease onset.

In separate experiments using these mice, we transferred (1–5 × 10^6, i.v.) sorted populations of MOG-specific CD4$^+$ Ag-experienced 2D2 T cells (CD44$^+$CD62L$^-$CD4$^+$ Vβ11$^+$ Dsred$^+$ Thy1.1$^-$, isolated from $MOG_{35–55}$–immunized mice) and naive 2D2 T cells (CD44$^-$CD62L$^+$CD4$^+$ Vβ11$^+$ Dsred$^-$ Thy1.1$^+$, isolated from unimmunized mice), which had been fluorescently labeled with Violet Cell Trace to track proliferation. T cell populations were transferred into MHC class II$^{-/-}$:CD11c-DTR and MHC class II$^{+/+}$:CD11c-DTR mixed BM chimera mice 1 d following the first administration of DT (DPI 9) to ensure DC ablation. At peak disease (DPI 16), immune cells were isolated from CNS and PLO tissues, and accumulation and proliferation of transferred naive (CD4$^+$ Vβ11$^+$ Thy1.1$^+$ Dsred$^-$) and Ag-experienced (CD4$^+$ Vβ11$^+$ Thy1.1$^-$ Dsred$^+$) 2D2 T cells were analyzed by flow cytometry (gating shown in Fig. 6F). As shown, transferred naive T cells displayed minimal proliferation in CNS or PLO tissues, and no difference in frequency of proliferated cells was observed between DT-treated and PBS-treated mice. However, we did observe a reduction in the frequency of total unproliferated cells in both spleens and cLNs of mice in which MHC class II$^{+/+}$ DCs had been ablated by DT treatment, indicating—not surprisingly—that MHC class II$^+$ DCs are required for survival of circulating naive donor T cells. More importantly, whereas the frequency of proliferated Ag-experienced 2D2 T cells was not statistically different in either cLNs or spleens of PBS- or DT-treated mice, ablation of MHC class II$^{+/+}$ DCs profoundly diminished the CNS recruitment of transferred MOG-specific Ag-experienced CD4$^+$ T cells ($p = 0.0096$, Fig. 6E). In summary, these data together with our previous findings support the conclusion that CCR2-dependent recruitment of CD11c$^+$ DCs to

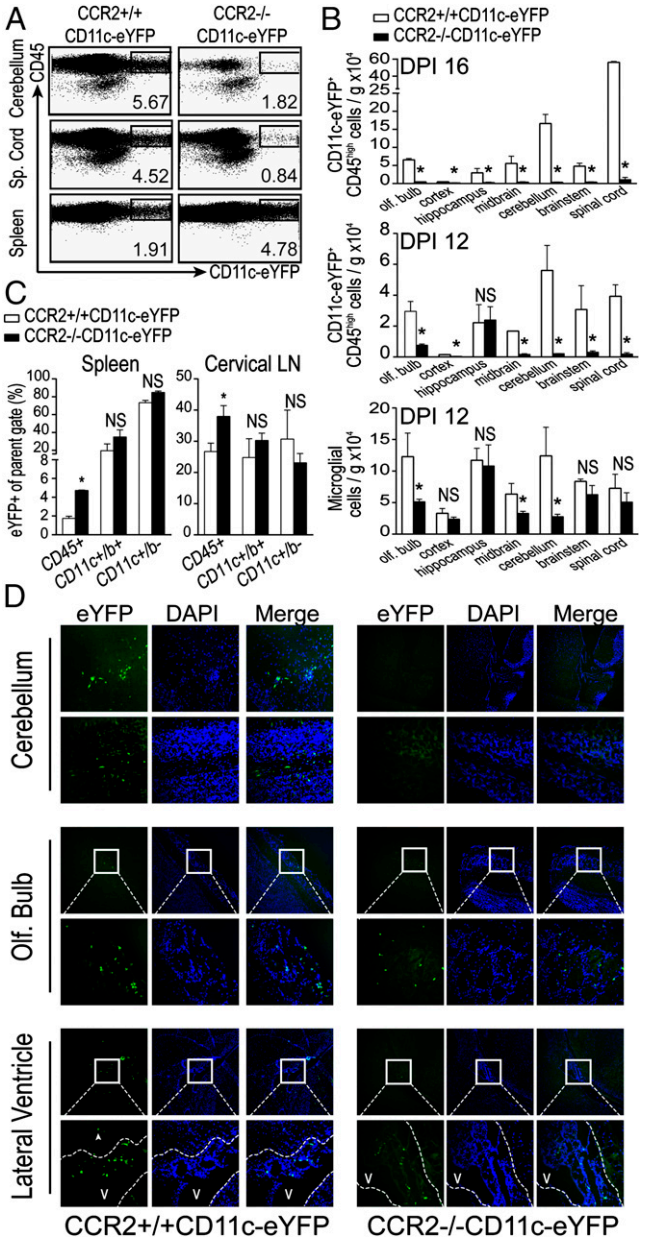

FIGURE 4. Deficient CNS accumulation of CCR2$^{-/-}$ CD11c-eYFP^{+} DCs in mixed BM chimeras. (**A**) Flow plots showing frequency of CD45^{high}CD11c-eYFP^{+} in cerebellum, spinal cord, and spleen at day 12 of EAE in mixed BM chimera mice receiving CCR2$^{+/+}$CD11c-eYFP or CCR2$^{-/-}$CD11c-eYFP BM cells. (**B**) Total number of CD45-high CD11c-eYFP^{+} cells and number of microglia (CD11b^{+}CD45-low cells) per gram tissue in the indicated CNS regions at days 12 and 16 EAE in CCR2$^{+/+}$ CD11c-eYFP and CCR2$^{-/-}$CD11c-eYFP BM recipients. (**C**) Frequency of CD11c^{+} cells among CD45^{+}, CD45^{+}CD11b^{+}, and CD45^{+}CD11b^{-} cell populations from spleen and cervical lymph node of CCR2$^{+/+}$CD11c-eYFP and CCR2$^{-/-}$CD11c-eYFP BM recipients at day 12 of EAE. (**D**) Fluorescent micrographs from CCR2$^{+/+}$CD11c-eYFP and CCR2$^{-/-}$CD11c-eYFP BM recipient chimeric mice depicting CD11c-eYFP^{+} cell accumulation in cerebellum, olfactory bulb, and tissue surrounding the lateral ventricle. Boxes indicate region magnified below. Low magnification images, ×40; high magnification images, ×100. Error bars indicate SEM. *$p < 0.05$, Student t test.

the CNS during onset of EAE contributes to disease progression by supporting the CNS recruitment of Ag-experienced encephalitogenic T cells and production of inflammatory cytokines by these cells through MHC class II–dependent in situ restimulation.

Discussion

Building on previous work demonstrating the importance of CCR2/CCL2 axis in neuroinflammation (20, 22, 29, 31–33, 43, 44), to our knowledge, we show for the first time that CCR2 is essential for DC recruitment to the CNS during EAE. Specifically, we show that, unlike for monocytes, CCR2 might not be essential for emigration of DC from BM, as CCR2$^{-/-}$ DCs were found in blood and spleen in mixed BM chimera mice. However, despite their

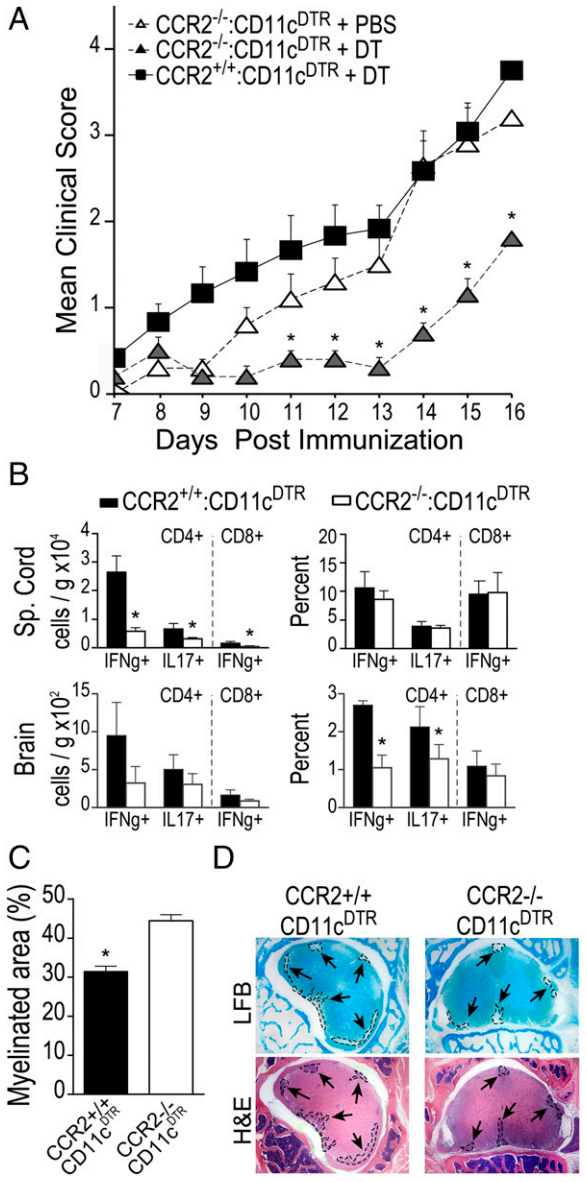

FIGURE 5. Ablation of CCR2$^{+/+}$ DCs during EAE clinical onset delays disease progression. (**A**) Mean clinical scores following MOG$_{35–55}$ immunization induced EAE shown for groups of WT mice (n = 5) reconstituted with mixtures of BM cells from the indicated donors. Mice were treated with DT (625 ng/kg, i.p.) or PBS on DPI 8, 10, and 12. (**B**) Total number (per gram tissue) and frequency of CNS-infiltrating CD4^{+} and CD8^{+} T cells expressing the indicated cytokines after 5-h ex vivo restimulation with PMA/ionomycin in DT-treated mice. (**C**) Spinal cord demyelination expressed as percentage of total cross-sectional area still myelinated at day 16 EAE (n = 5 mice per group). (**D**) Luxol fast blue (LFB) and H&E-stained micrographs of spinal cord tissue from DT-treated CCR2$^{+/+}$:CD11c-DTR and CCR2$^{-/-}$:CD11c-DTR recipient mixed BM chimeric mice with EAE (DPI 16). Arrows indicate inflammatory foci (outlined with dashed lines, *bottom*) and demyelinated lesions (outlined with dashed lines, *top*). Error bars indicate SEM. *$p < 0.05$, Student t test.

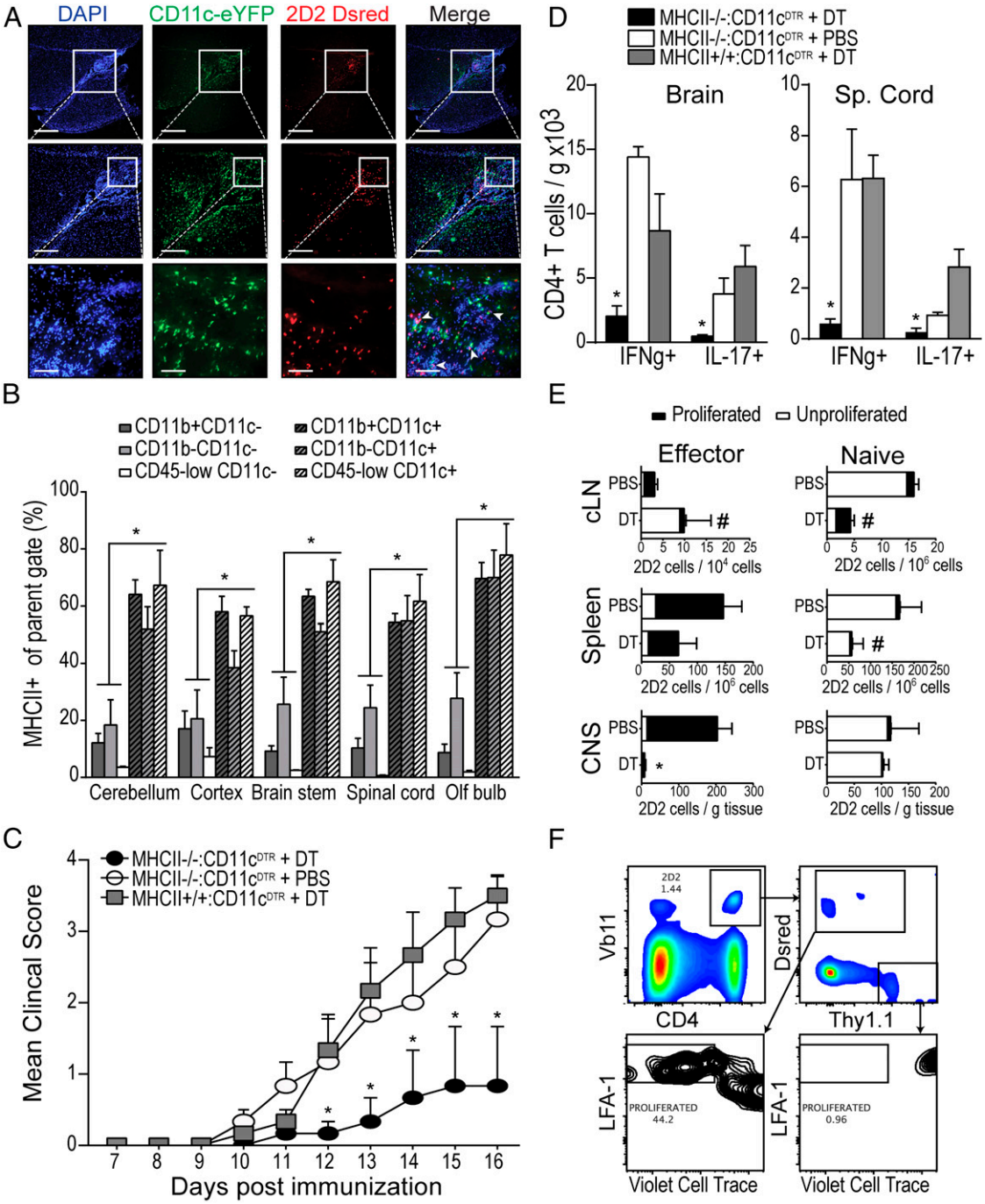

FIGURE 6. MHC class II expression on CNS-infiltrating DCs contributes to proliferation, recruitment, and cytokine production by coinfiltrating, myelin-specific effector T cells. (**A**) Fluorescent micrographs of DAPI-stained sagittal brain sections showing developing periventricular inflammatory lesions in CD11c-eYFP mice after adoptive transfer of purified $CD4^+$ MOG-specific 2D2.Dsred T cells and EAE induction (DPI 12). $CD11c\text{-}eYFP^+$ cells shown in green. The 2D2.Dsred T cells are shown in red. Scale bars, 700 μm (*top row*), 280 μm (*middle row*), and 70 (*bottom row*). (**B**) Frequency of MHC class II–expressing cells among various $CD11c^+$ and $CD11c^-$ cell subsets isolated from CNS of CD11c-eYFP mice with EAE (DPI 12). (**C**) Mean EAE clinical score is shown for groups ($n = 3$) of WT mice reconstituted with mixtures of BM cells from the indicated donors. Mice were treated with DT (625 ng/kg, i.p.) or PBS on DPI 8, 10, 12, and 14. (**D**) Total number (per gram tissue) of spinal cord–infiltrating $CD4^+$ T cells that produced IFN-γ or IL-17 following 5-h ex vivo restimulation with $MOG_{35–55}$ peptide (20 μg/ml). (**E**) Pure FACS-sorted populations of MOG-specific naive 2D2.Thy1.1 ($CD4^+$ $V\beta11^+$ $CD62L^+$ $CD44^-$ $Thy1.1^+$ $Dsred^-$) or Ag-experienced 2D2.Dsred ($CD4^+$ $V\beta11^+$ $CD62L^-$ $CD44^+$ $Thy1.1^-$ $Dsred^+$) T cells were mixed together, labeled with Violet Cell Trace, and adoptively transferred into congenic MHC $II^{-/-}$:CD11c-DTR mice with EAE (DPI 9). Recipient mice were treated with either DT (625 ng/kg, i.p.) or PBS on DPI 8, 10, 12, and 14. Bar graphs show frequency of proliferated (LFA1-high Violet Cell Trace-low) and unproliferated (LFA1-low Violet Cell Trace-high) transferred 2D2 T cells in cervical lymph node, spleen, and CNS tissues (expressed per gram tissue). Gating of transferred cells is shown in (**F**). Error bars indicate SEM. $^*p < 0.05$, $^\#p < 0.1$, Student *t* test.

abundance in blood and peripheral lymphoid organ tissues, $CCR2^{-/-}$ DCs failed to accumulate in the inflamed CNS, suggesting that CCR2 directly contributes to DC migration from blood to CNS tissues. We also show that CCR2-dependent DC migration into the inflamed CNS is essential for disease progression during the early effector phase of EAE and that CNS-

infiltrating DCs contribute to this progression by presenting Ag to encephalitogenic $CD4^+$ T cells in the context of MHC class II.

Several studies have shown that DCs contribute to demyelinating lesion formation by promoting T cell activation and infiltration of the parenchyma through multiple mechanisms, including breakdown of the glia limitans (45, 46), chemokine secretion (47–49), and MHC- and cofactor-dependent restimulation (2, 3, 11, 18, 36, 37, 39, 50–52). To enter CNS parenchyma, perivascular cells must cross the glia-limitans and its associated basement membrane. Matrix metalloproteinases (MMPs), especially MMP-9 and MMP-2, which are required for EAE clinical onset, have been shown to contribute to breakdown of dystro-glycan linkages between astroglial end feet and the glia limitans basal lamina (45). These MMPs are thought to be produced by perivascular myeloid cells. We have shown that, upon transmigrating across brain microvessel endothelial cells in vitro, DCs upregulate expression of MMP9 and MMP2 (46), suggesting that this might be one mechanism by which DCs promoted infiltration into the CNS parenchyma during EAE. Others demonstrated that human monocytes transform into DCs upon in vitro migration across artificial blood brain barriers and upregulate expression of the cytokines TGF-β and IL-6, which might promote differentiation of coinfiltrating effector T cells into inflammatory Th17 cells (50). Tissue DCs also produce T cell–attracting chemokines (53), and in murine glioma models have been shown to attract cytotoxic T cells to the tumor microenvironment through CXCL10 (47). Additionally, DCs producing CXCL13 have been detected in ectopic lymphoid structures in the cerebral meninges of patients with secondary progressive multiple sclerosis (MS) (48) and in mice with EAE (49), which may attract T cells or promote DC–T cell clustering and contact-dependent interactions in the perivascular space.

Despite the extensive knowledge describing the important role of DCs in initiating CNS neuroinflammation, the exact mechanism regarding their migration into the CNS is less known. In this work, we demonstrate that CCR2-mediated migration is critical for DC accumulation in the CNS and provide further evidence that CNS DCs promote EAE disease progression through MHC class II–dependent restimulation of effector T cells. CNS-infiltrating T cells must re-encounter their cognate Ag in the context of MHC molecules to carry out effector functions, such as cytokine secretion. In seminal experiments, Greter et al. (3) have shown that restricting Ag presentation by MHC class II to BM-derived $CD11c^+$ cells is sufficient for EAE onset and progression. In this study, we propose that infiltrating $CD11c^+$ cells are not only sufficient, but also required for T cell restimulation during EAE disease onset. Consistent with our data, ex vivo assays have shown that CNS myeloid DCs—although not macrophages or microglia—present endogenously acquired myelin Ags to T cells and drive effector T cell differentiation (1, 11). More recently, Wlodarczyk et al. (42) have shown that, during EAE, $CD11c^+$ cells found in the CNS include both infiltrating $CD11c^+$ cells and $CD11c^+$ microglia. They further showed that, unlike $CD11c^-$ microglia, $CD11c^+$ microglia expressed MHC class II and were capable of stimulating proliferation of myelin-specific T cells. However, compared with infiltrating $CD11c^+$ cells, these cells were deficient in their expression of third-signal cytokines necessary for driving Th1 and Th17 cell differentiation, including IL-1β, IL-12, IL-6, and IL-23, and favored Th2 and T regulatory differentiation instead. Interestingly, they also showed that infiltrating $CD11c^+$ cells expressed higher levels of CCR2 than $CD11c^+$ or $CD11c^-$ microglia. Additionally, recent work has shown that DC–T cell interactions in the CNS are important for cross presentation of CNS Ags to $CD8^+$ T cells (18) and epitope spreading among $CD4^+$ T cells (2), both of which are thought to contribute to MS disease progression. In humans, MHC class II^+ DCs are present in demyelinating MS lesions, where they have been shown to acquire myelin debris and interact with proliferating T cells (52). Taken together, these studies strongly imply a central role for CNS DCs in driving T cell restimulation in situ. This hypothesis is further supported by studies using the adoptive transfer EAE model, in which i.v. delivery of myelin Ag during initial T cell entry into the CNS promoted local T cell activation and exacerbated disease (54). The CNS-specific effect of this study was confirmed by intravital imaging of myelin-specific T cells in meningeal tissue, in which Pesic et al. (39) noted increased T cell infiltration into parenchyma following intrathecal injection of Ag-pulsed DCs.

Similarly, we previously demonstrated that, during EAE, intracerebral injection of myelin Ag-pulsed DCs exacerbates disease and promotes MOG-specific T cell recruitment, cytokine production, and proliferation (34). In line with these data, our present studies show that depleting DCs during EAE disease onset delays disease progression. In contrast, others have previously shown that $CD11c^+$ DCs may be dispensable during the priming phase of EAE (day 0–10) (55). We show similarly that depletion of $CD11c^+$ cells after disease onset does not support recovery—suggesting an important window period during the early effector phase of EAE in which DCs are required for onset of neuroinflammation. Outside this window, it is likely that $CD11c^+$ cell functions are nonrate limiting and/or redundant with other APCs such as B cells, macrophages, or other $CD11c^-$ DC populations. Moreover, these findings could imply that DCs play different, potentially redundant and nonredundant roles during distinct phases of EAE pathogenesis. Indeed, in our hands, depletion of DCs at later time points tended to worsen EAE or slow recovery, perhaps due to the presence of a tolerogenic DC population during the recovery phase. This is consistent with previous reports in which DCs isolated from CNS during EAE onset stimulated robust Th1 and Th17 responses, whereas DCs isolated at later time points were inefficient APCs that supported regulatory T cell–mediated suppression (1, 56, 57).

A nonredundant pathogenic role of $CD11c^+$ DCs during EAE onset is consistent with previous work in which reducing the number of circulating DCs indirectly by neutralizing the DC growth factor FLT3L ameliorated EAE (58). Conversely, Greter et al. (3) showed that EAE clinical disease is exacerbated when the level of circulating DCs is increased by i.v. administration of FLT3L.Ig, and others have shown that FLT3L administration causes spontaneous EAE in transgenic mice constitutively expressing CCL2 in CNS tissues. We show similarly that directly increasing the level of circulating DCs during active disease by i.v. transfer of high numbers of $CCR2^{+/+}$ BMDCs accelerates disease progression. We also show that transient ablation of $CCR2^{+/+}$ or MHC class $II^{+/+}$ DCs ameliorates disease—suggesting that the observed DC contribution to EAE disease progression at this time point is dependent upon both CCR2-mediated recruitment to effector tissues and MHC class II–mediated restimulation of Ag-experienced T cells within the CNS.

In summary, our findings suggest that targeted strategies that inhibit the CCR2-dependent migratory capacity or MHC class II–dependent Ag-presentation capacity of circulating DCs may be beneficial during acute neuroinflammatory episodes or relapses in CNS autoimmune disease. Because CCR2 contributes to an array of cell migration events in vivo, selective targeting of circulating DCs would be crucial to minimizing potential side effects of CCR2 inhibitors. Future work should focus on exploring the therapeutic potential of CCR2 inhibition using selective delivery systems that target DCs, as well as identifying molecules that specifically contribute to DC migration across the blood brain barrier.

Acknowledgments

We thank Satoshi Kinoshita for expert histopathology services and members of our laboratory for helpful discussions and constructive criticisms of this work. We also thank Khen Macvilay for expertise provided for cytofluorimetry.

Disclosures

The authors have no financial conflicts of interest.

References

1. Juedes, A. E., and N. H. Ruddle. 2001. Resident and infiltrating central nervous system APCs regulate the emergence and resolution of experimental autoimmune encephalomyelitis. *J. Immunol.* 166: 5168–5175.
2. McMahon, E. J., S. L. Bailey, C. V. Castenada, H. Waldner, and S. D. Miller. 2005. Epitope spreading initiates in the CNS in two mouse models of multiple sclerosis. *Nat. Med.* 11: 335–339.
3. Greter, M., F. L. Heppner, M. P. Lemos, B. M. Odermatt, N. Goebels, T. Laufer, R. J. Noelle, and B. Becher. 2005. Dendritic cells permit immune invasion of the CNS in an animal model of multiple sclerosis. *Nat. Med.* 11: 328–334.
4. Bulloch, K., M. M. Miller, J. Gal-Toth, T. A. Milner, A. Gottfried-Blackmore, E. M. Waters, U. W. Kaunzner, K. Liu, R. Lindquist, M. C. Nussenzweig, et al. 2008. CD11c/EYFP transgene illuminates a discrete network of dendritic cells within the embryonic, neonatal, adult, and injured mouse brain. *J. Comp. Neurol.* 508: 687–710.
5. Gottfried-Blackmore, A., U. W. Kaunzner, J. Idoyaga, J. C. Felger, B. S. McEwen, and K. Bulloch. 2009. Acute in vivo exposure to interferon-gamma enables resident brain dendritic cells to become effective antigen presenting cells. *Proc. Natl. Acad. Sci. USA* 106: 20918–20923.
6. Felger, J. C., T. Abe, U. W. Kaunzner, A. Gottfried-Blackmore, J. Gal-Toth, B. S. McEwen, C. Iadecola, and K. Bulloch. 2010. Brain dendritic cells in ischemic stroke: time course, activation state, and origin. *Brain Behav. Immun.* 24: 724–737.
7. D'Agostino, P. M., C. Kwak, H. A. Vecchiarelli, J. G. Toth, J. M. Miller, Z. Masheeb, B. S. McEwen, and K. Bulloch. 2012. Viral-induced encephalitis initiates distinct and functional CD103+ CD11b+ brain dendritic cell populations within the olfactory bulb. *Proc. Natl. Acad. Sci. USA* 109: 6175–6180.
8. Kaunzner, U. W., M. M. Miller, A. Gottfried-Blackmore, J. Gal-Toth, J. C. Felger, B. S. McEwen, and K. Bulloch. 2012. Accumulation of resident and peripheral dendritic cells in the aging CNS. *Neurobiol. Aging* 33: 681-693.e1.
9. Karman, J., C. Ling, M. Sandor, and Z. Fabry. 2004. Initiation of immune responses in brain is promoted by local dendritic cells. *J. Immunol.* 173: 2353–2361.
10. Newman, T. A., I. Galea, N. van Rooijen, and V. H. Perry. 2005. Blood-derived dendritic cells in an acute brain injury. *J. Neuroimmunol.* 166: 167–172.
11. Bailey, S. L., B. Schreiner, E. J. McMahon, and S. D. Miller. 2007. CNS myeloid DCs presenting endogenous myelin peptides 'preferentially' polarize CD4+ T (H)-17 cells in relapsing EAE. *Nat. Immunol.* 8: 172–180.
12. Fischer, H. G., U. Bonifas, and G. Reichmann. 2000. Phenotype and functions of brain dendritic cells emerging during chronic infection of mice with *Toxoplasma gondii*. *J. Immunol.* 164: 4826–4834.
13. Fischer, H. G., and G. Reichmann. 2001. Brain dendritic cells and macrophages/microglia in central nervous system inflammation. *J. Immunol.* 166: 2717–2726.
14. Reichmann, G., M. Schroeter, S. Jander, and H. G. Fischer. 2002. Dendritic cells and dendritic-like microglia in focal cortical ischemia of the mouse brain. *J. Neuroimmunol.* 129: 125–132.
15. Serafini, B., S. Columba-Cabezas, F. Di Rosa, and F. Aloisi. 2000. Intracerebral recruitment and maturation of dendritic cells in the onset and progression of experimental autoimmune encephalomyelitis. *Am. J. Pathol.* 157: 1991–2002.
16. Jain, P., C. Coisne, G. Enzmann, R. Rottapel, and B. Engelhardt. 2010. Alpha4beta1 integrin mediates the recruitment of immature dendritic cells across the blood-brain barrier during experimental autoimmune encephalomyelitis. *J. Immunol.* 184: 7196–7206.
17. Miller, S. D., E. J. McMahon, B. Schreiner, and S. L. Bailey. 2007. Antigen presentation in the CNS by myeloid dendritic cells drives progression of relapsing experimental autoimmune encephalomyelitis. *Ann. N. Y. Acad. Sci.* 1103: 179–191.
18. Ji, Q., L. Castelli, and J. M. Goverman. 2013. MHC class I-restricted myelin epitopes are cross-presented by Tip-DCs that promote determinant spreading to $CD8^+$ T cells. *Nat. Immunol.* 14: 254–261.
19. Vanbervliet, B., B. Homey, I. Durand, C. Massacrier, S. Aït-Yahia, O. de Bouteiller, A. Vicari, and C. Caux. 2002. Sequential involvement of CCR2 and CCR6 ligands for immature dendritic cell recruitment: possible role at inflamed epithelial surfaces. *Eur. J. Immunol.* 32: 231–242.
20. Sagar, D., A. Lamontagne, C. A. Foss, Z. K. Khan, M. G. Pomper, and P. Jain. 2012. Dendritic cell CNS recruitment correlates with disease severity in EAE via CCL2 chemotaxis at the blood-brain barrier through paracellular transmigration and ERK activation. *J. Neuroinflammation* 9: 245.
21. Osterholzer, J. J., J. L. Curtis, T. Polak, T. Ames, G. H. Chen, R. McDonald, G. B. Huffnagle, and G. B. Toews. 2008. CCR2 mediates conventional dendritic cell recruitment and the formation of bronchovascular mononuclear cell infiltrates in the lungs of mice infected with *Cryptococcus neoformans*. *J. Immunol.* 181: 610–620.
22. Fife, B. T., G. B. Huffnagle, W. A. Kuziel, and W. J. Karpus. 2000. CC chemokine receptor 2 is critical for induction of experimental autoimmune encephalomyelitis. *J. Exp. Med.* 192: 899–905.
23. Park, S. J., M. D. Burdick, W. K. Brix, M. H. Stoler, D. S. Askew, R. M. Strieter, and B. Mehrad. 2010. Neutropenia enhances lung dendritic cell recruitment in response to *Aspergillus* via a cytokine-to-chemokine amplification loop. *J. Immunol.* 185: 6190–6197.
24. Charbonnier, A. S., N. Kohrgruber, E. Kriehuber, G. Stingl, A. Rot, and D. Maurer. 1999. Macrophage inflammatory protein 3alpha is involved in the constitutive trafficking of epidermal Langerhans cells. *J. Exp. Med.* 190: 1755–1768.
25. Piemonti, L., B. E. Leone, R. Nano, A. Saccani, P. Monti, P. Maffi, G. Bianchi, A. Sica, G. Peri, R. Melzi, et al. 2002. Human pancreatic islets produce and secrete MCP-1/CCL2: relevance in human islet transplantation. *Diabetes* 51: 55–65.
26. Page, G., S. Lebecque, and P. Miossec. 2002. Anatomic localization of immature and mature dendritic cells in an ectopic lymphoid organ: correlation with selective chemokine expression in rheumatoid synovium. *J. Immunol.* 168: 5333–5341.
27. Chabaud, M., G. Page, and P. Miossec. 2001. Enhancing effect of IL-1, IL-17, and TNF-alpha on macrophage inflammatory protein-3alpha production in rheumatoid arthritis: regulation by soluble receptors and Th2 cytokines. *J. Immunol.* 167: 6015–6020.
28. Toft-Hansen, H., R. Buist, X. J. Sun, A. Schellenberg, J. Peeling, and T. Owens. 2006. Metalloproteinases control brain inflammation induced by pertussis toxin in mice overexpressing the chemokine CCL2 in the central nervous system. *J. Immunol.* 177: 7242–7249.
29. Jee, Y., W. K. Yoon, Y. Okura, N. Tanuma, and Y. Matsumoto. 2002. Upregulation of monocyte chemotactic protein-1 and CC chemokine receptor 2 in the central nervous system is closely associated with relapse of autoimmune encephalomyelitis in Lewis rats. *J. Neuroimmunol.* 128: 49–57.
30. Savarin, C., S. A. Stohlman, R. Atkinson, R. M. Ransohoff, and C. C. Bergmann. 2010. Monocytes regulate T cell migration through the glia limitans during acute viral encephalitis. *J. Virol.* 84: 4878–4888.
31. Dogan, R. N., A. Elhofy, and W. J. Karpus. 2008. Production of CCL2 by central nervous system cells regulates development of murine experimental autoimmune encephalomyelitis through the recruitment of TNF- and iNOS-expressing macrophages and myeloid dendritic cells. *J. Immunol.* 180: 7376–7384.
32. Izikson, L., R. S. Klein, I. F. Charo, H. L. Weiner, and A. D. Luster. 2000. Resistance to experimental autoimmune encephalomyelitis in mice lacking the CC chemokine receptor (CCR)2. *J. Exp. Med.* 192: 1075–1080.
33. Gaupp, S., D. Pitt, W. A. Kuziel, B. Cannella, and C. S. Raine. 2003. Experimental autoimmune encephalomyelitis (EAE) in $CCR2(^{-/-})$ mice: susceptibility in multiple strains. *Am. J. Pathol.* 162: 139–150.
34. Zozulya, A. L., S. Ortler, J. Lee, C. Weidenfeller, M. Sandor, H. Wiendl, and Z. Fabry. 2009. Intracerebral dendritic cells critically modulate encephalitogenic versus regulatory immune responses in the CNS. *J. Neurosci.* 29: 140–152.
35. Fleming, K. K., J. A. Bovaird, M. C. Mosier, M. R. Emerson, S. M. LeVine, and J. G. Marquis. 2005. Statistical analysis of data from studies on experimental autoimmune encephalomyelitis. *J. Neuroimmunol.* 170: 71–84.
36. Bartholomäus, I., N. Kawakami, F. Odoardi, C. Schläger, D. Miljkovic, J. W. Ellwart, W. E. Klinkert, C. Flügel-Koch, T. B. Issekutz, H. Wekerle, and A. Flügel. 2009. Effector T cell interactions with meningeal vascular structures in nascent autoimmune CNS lesions. *Nature* 462: 94–98.
37. Kivisäkk, P., J. Imitola, S. Rasmussen, W. Elyaman, B. Zhu, R. M. Ransohoff, and S. J. Khoury. 2009. Localizing central nervous system immune surveillance: meningeal antigen-presenting cells activate T cells during experimental autoimmune encephalomyelitis. *Ann. Neurol.* 65: 457–469.
38. Hickey, W. F., and H. Kimura. 1988. Perivascular microglial cells of the CNS are bone marrow-derived and present antigen in vivo. *Science* 239: 290–292.
39. Pesic, M., I. Bartholomäus, N. I. Kyratsous, V. Heissmeyer, H. Wekerle, and N. Kawakami. 2013. 2-photon imaging of phagocyte-mediated T cell activation in the CNS. *J. Clin. Invest.* 123: 1192–1201.
40. Clarkson, B. D., E. Héninger, M. G. Harris, J. Lee, M. Sandor, and Z. Fabry. 2012. Innate-adaptive crosstalk: how dendritic cells shape immune responses in the CNS. *Adv. Exp. Med. Biol.* 946: 309–333.
41. Becher, B., I. Bechmann, and M. Greter. 2006. Antigen presentation in autoimmunity and CNS inflammation: how T lymphocytes recognize the brain. *J. Mol. Med.* 84: 532–543.
42. Wlodarczyk, A., M. Løbner, O. Cédile, and T. Owens. 2014. Comparison of microglia and infiltrating $CD11c^+$ cells as antigen presenting cells for T cell proliferation and cytokine response. *J. Neuroinflammation* 11: 57.
43. Furtado, G. C., B. Piña, F. Tacke, S. Gaupp, N. van Rooijen, T. M. Moran, G. J. Randolph, R. M. Ransohoff, S. W. Chensue, C. S. Raine, and S. A. Lira. 2006. A novel model of demyelinating encephalomyelitis induced by monocytes and dendritic cells. *J. Immunol.* 177: 6871–6879.
44. Schellenberg, A. E., R. Buist, M. R. Del Bigio, H. Toft-Hansen, R. Khorooshi, T. Owens, and J. Peeling. 2012. Blood-brain barrier disruption in CCL2 transgenic mice during pertussis toxin-induced brain inflammation. *Fluids Barriers CNS* 9: 10.
45. Agrawal, S., P. Anderson, M. Durbeej, N. van Rooijen, F. Ivars, G. Opdenakker, and L. M. Sorokin. 2006. Dystroglycan is selectively cleaved at the parenchymal basement membrane at sites of leukocyte extravasation in experimental autoimmune encephalomyelitis. *J. Exp. Med.* 203: 1007–1019.
46. Zozulya, A. L., E. Reinke, D. C. Baiu, J. Karman, M. Sandor, and Z. Fabry. 2007. Dendritic cell transmigration through brain microvessel endothelium is regulated by MIP-1alpha chemokine and matrix metalloproteinases. *J. Immunol.* 178: 520–529.

47. Fujita, M., X. Zhu, R. Ueda, K. Sasaki, G. Kohanbash, E. R. Kastenhuber, H. A. McDonald, G. A. Gibson, S. C. Watkins, R. Muthuswamy, et al. 2009. Effective immunotherapy against murine gliomas using type 1 polarizing dendritic cells—significant roles of CXCL10. *Cancer Res.* 69: 1587–1595.
48. Serafini, B., B. Rosicarelli, R. Magliozzi, E. Stigliano, and F. Aloisi. 2004. Detection of ectopic B-cell follicles with germinal centers in the meninges of patients with secondary progressive multiple sclerosis. *Brain Pathol.* 14: 164–174.
49. Magliozzi, R., S. Columba-Cabezas, B. Serafini, and F. Aloisi. 2004. Intracerebral expression of CXCL13 and BAFF is accompanied by formation of lymphoid follicle-like structures in the meninges of mice with relapsing experimental autoimmune encephalomyelitis. *J. Neuroimmunol.* 148: 11–23.
50. Ifergan, I., H. Kebir, M. Bernard, K. Wosik, A. Dodelet-Devillers, R. Cayrol, N. Arbour, and A. Prat. 2008. The blood-brain barrier induces differentiation of migrating monocytes into Th17-polarizing dendritic cells. *Brain: a journal of neurology* 131: 785-799.
51. Kawakami, N., U. V. Nägerl, F. Odoardi, T. Bonhoeffer, H. Wekerle, and A. Flügel. 2005. Live imaging of effector cell trafficking and autoantigen recognition within the unfolding autoimmune encephalomyelitis lesion. *J. Exp. Med.* 201: 1805–1814.
52. Serafini, B., B. Rosicarelli, R. Magliozzi, E. Stigliano, E. Capello, G. L. Mancardi, and F. Aloisi. 2006. Dendritic cells in multiple sclerosis lesions: maturation stage, myelin uptake, and interaction with proliferating T cells. *J. Neuropathol. Exp. Neurol.* 65: 124–141.
53. Tang, H. L., and J. G. Cyster. 1999. Chemokine up-regulation and activated T cell attraction by maturing dendritic cells. *Science* 284: 819–822.
54. Odoardi, F., N. Kawakami, W. E. Klinkert, H. Wekerle, and A. Flügel. 2007. Blood-borne soluble protein antigen intensifies T cell activation in autoimmune CNS lesions and exacerbates clinical disease. *Proc. Natl. Acad. Sci. USA* 104: 18625–18630.
55. Isaksson, M., B. A. Lundgren, K. M. Ahlgren, O. Kämpe, and A. Lobell. 2012. Conditional DC depletion does not affect priming of encephalitogenic Th cells in EAE. *Eur. J. Immunol.* 42: 2555–2563.
56. Deshpande, P., I. L. King, and B. M. Segal. 2007. Cutting edge: CNS CD11c+ cells from mice with encephalomyelitis polarize Th17 cells and support CD25+CD4+ T cell-mediated immunosuppression, suggesting dual roles in the disease process. *J. Immunol.* 178: 6695–6699.
57. Suter, T., G. Biollaz, D. Gatto, L. Bernasconi, T. Herren, W. Reith, and A. Fontana. 2003. The brain as an immune privileged site: dendritic cells of the central nervous system inhibit T cell activation. *Eur. J. Immunol.* 33: 2998–3006.
58. Whartenby, K. A., P. A. Calabresi, E. McCadden, B. Nguyen, D. Kardian, T. Wang, C. Mosse, D. M. Pardoll, and D. Small. 2005. Inhibition of FLT3 signaling targets DCs to ameliorate autoimmune disease. *Proc. Natl. Acad. Sci. USA* 102: 16741–16746.

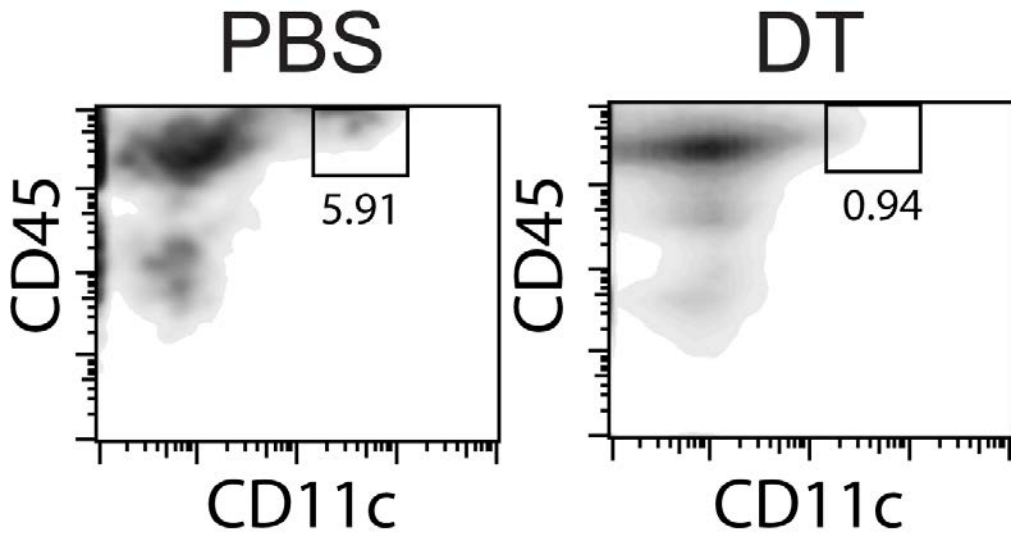

Supplemental Figure 1.

Following MOG_{35-55} immunization CD11c-DTR mice were injected with DT (625ng / kg, i.p.) or PBS on day 14, 16, 18, and 20 of EAE. Two days following the last injection immune cells were isolated from CNS tissues, stained for CD45 and CD11c, and depletion efficiency was evaluated by flow cytometry. Numbers indicate percentage of cells in boxed gate.